ARTICLE

Clay-Supported Molybdenum-Based Catalysts for Higher Alcohol Synthesis from Syngas

Gai-mei Wu[a], Ji-long Zhou[b], Mei-mei Lv[b], Wei Xie[b], Song Sun[b], Chen Gao[b], Wen-dong Wang[a*], Jun Bao[b*]

a. Department of Chemical Physics, University of Science and Technology of China, Hefei 230026, China
b. National Synchrotron Radiation Laboratory, University of Science and Technology of China, Hefei 230029, China

(Dated: Received on April 17, 2015; Accepted on May 24, 2015)

A kind of clay-supported K-Co-Mo catalyst was prepared by a sol-gel method combined with incipient wetness impregnation. The catalyst structure was characterized by X-ray diffraction, N_2 adsorption-desorption, H_2 temperature-programmed reduction, and X-ray photoelectron spectroscopy techniques and its catalytic performance for higher alcohol synthesis from syngas was investigated. The active components has a high dispersion on the clay support surface. The increase of the Mo loading promoted reduction of Mo^{6+} but had no significant influence on the reduction of Mo^{4+} and Co^{2+} species. After reduction, a kind of lower state $Mo^{\delta+}$ ($1<\delta<4$) species was observed on the surface. Compared with the unsupported catalyst, the clay supported K-Co-Mo catalysts showed much higher catalytic performance for alcohol formation. The reason can be explained that the supported catalyst have a high active surface area and the mesoporous structure prolonged the residence time of intermediates for alcohol formation to some extent, which promoted the formation of higher alcohols. The high activity of the catalyst reduced at 773 K may be attributed to the high content of $Mo^{\delta+}$ ($1<\delta<4$) species on the surface, which was regarded as the active site for the adsorption of nondissociative CO and responsible for the alcohol formation.

Key words: Higher alcohol synthesis, Clay support, K-Co-Mo catalyst, Syngas

I. INTRODUCTION

Owing to the increasing seriousness of environmental concerns and the exhaustion of the non-renewable fossil fuels, higher alcohol synthesis from syngas has attracted considerable attentions in recent years. Higher alcohol such as ethanol, isopropanol, can be used as high-octane gasoline and chemical raw materials [1]. Several catalytic systems, such as modified methanol catalysts, modified F-T synthesis catalysts and modified Mo-based catalysts, have been developed for higher alcohol synthesis [2, 3]. Among these, alkali promoted molybdenum based catalysts have attracted more attentions due to the excellent resistance to sulfur poisoning property [4, 5]. The addition of alkali metal can suppress the hydrogenation ability [6], reduce the surface acidity and thus benefit for the formation of higher alcohols.

The addition of some transition metals, especially Co, can further increase the alcohol production [7]. The Co promotion to reduced K-Mo/Al_2O_3 and K-Mo/SiO_2 catalysts increased the activity toward the formation of higher alcohol due to the strong interaction between Co promoter and Mo species [8]. Similar result was obtained over the K-Mo_2C catalysts [9]. For the MoS_2 catalysts, the modification of Co promoted chain growth, leading to $C_{2+}OH$ formation [10]. The Co species operated as a synergistic system with the MoS_2 phase, rather than being independent of the MoS_2 phase [11]. The "Co-Mo-S" phase was regarded as the active species for the alcohol synthesis. Beside Co, Ni and Rh were also found to be effective promoters for alkali-promoted Mo-based catalysts for higher alcohol synthesis [12, 13].

The texture and property of supports can influence the metal dispersion, degree of reduction and the interaction with active species and support. Some metal oxide, such as Al_2O_3, SiO_2, have been used as the supports for higher alcohol synthesis [14, 15]. However, the surface acidity of these oxide was unfavorable to form alcohols because of the alcohol dehydration on the acidic sites of supports and catalyst deactivation by coke formation [16, 17]. Carbon materials, such as activated carbon, carbon nanotubes, have been attracting attention as potential catalyst supports for higher alcohol s-

*Authors to whom correspondence should be addressed. E-mail: baoj@ustc.edu.cn, wangwd@ustc.edu.cn.

ynthesis from syngas [18]. The uniform metal distribution and high metal dispersions were observed on the MWCNT support, which performed excellent catalytic activity and stability for higher alcohol synthesis [19]. Besides, some aluminosilicate with special structure and property, such as H-ZSM-5, hydrotalcite *etc.*, were also used as the supports for the Mo-based catalysts [20]. Clays are abundant, cheap, and environmentally natural minerals with layered structure [21]. Clays, such as bentonite, montmorillonite, and hectorite, has been reported to be effective partial hydrogenation supports and used in various catalytic reactions [22, 23]. Iranmahboob *et al.* studied the clay-supported molybdenum sulfide catalysts, and found that the incorporation of clay increased the selectivity of C_{2+} alcohol and the yield of total alcohols [24, 25]. The K and Ni promoted MoS_2/Al_2O_3-montmorillonitecan get the 34.6% CO conversion and 33.5% selectivity for higher alcohol synthesis. Furthermore, Liu *et al.* also reported that the MoS_2 catalyst supported on montmorillonite possessed a high thermo stability [26].

In our previous work, a kind of reduced unsupported K-Co-Mo catalyst with uniform metals distribution and high dispersion was developed, which exhibited high activity for higher alcohol synthesis from syngas [27]. To further improve the catalytic performance, especially the $C_{2+}OH$ selectivity, in this work the clay was incorporated as the support to prepare the K-Co-Mo/clay catalysts. The structure was characterized by X-ray diffraction (XRD), N_2 physisorption, H_2 temperature-programmed reduction (H_2-TPR), and X-ray photoelectron spectroscopy (XPS). The activity of the catalyst for the synthesis of higher alcohols from syngas was investigated and the relationship between the structure and catalytic performance was discussed.

II. EXPERIMENTS

A. Catalyst preparation

The clay supported K-C-Mo catalysts were prepared by a sol-gel method combined with incipient wetness impregnation. The detailed procedure for preparing K-Co-Mo sol was described in our previous work [28]. All reagents were supplied by Sinopharm Chemical Reagent Co., Ltd. Before use, the clay was dried at 393 K for 3 h to remove the adsorbates on the surface. The as-prepared sol was impregnated into clay. The obtained mixture was dried at 393 K overnight, followed by calcination at 673 K in nitrogen for 4 h. The molar ratio of K/Mo and Co/Mo were 0.1 and 0.5, respectively. The Mo content in the samples, expressed as the Mo/clay weight ratio, ranged from 30% to 70%.

B. Catalyst characterization

XRD were obtained on a Rigaku TTR-III X-ray power diffractometer equipped with a Cu Kα radiation source at 40 kV in the range of $3°-80°$. TPR was performed on a Micromeritics AutoChem II 2920 instrument. For each analysis, approximately 50 mg of sample was loaded in a quartz reactor and heated in the temperature range from room temperature to 1173 K at a heating rate of 10 K/min in a stream of 5% H_2 in Ar with a flow rate of 50 mL/min. XPS analysis was performed on a Thermo ESCALAB 250 spectrometer using Al Kα ($h\nu$=1486.6 eV) as the X-ray source. The binding energy of C1s (284.5 eV) was used as a reference to correct the binding energy of the catalysts. Baseline correction was conducted by the Shirley method. Mo $3d_{5/2}$ and $3d_{3/2}$ peaks were separated by 3.15 eV with peak ratios of 3/2. All binding energies obtained in this work were within $\pm$0.2 eV.

C. Catalyst testing

The catalytic performance for higher alcohol synthesis from syngas was measured in a fixed-bed tubular stainless steel reactor with an internal diameter of 8 mm. For each experiment, 0.5 g catalyst mixed with quartz sand to make the total volume of 2 mL was loaded at the center of the reactor. The reaction temperature was controlled by a thermocouple placed exactly on the middle of the catalyst bed and visually monitored by a digital programmable controller. Prior to the reaction, the catalyst was *in situ* reduced in a mixed flow of H_2/N_2 ($5\%H_2$) at a flow rate of 40 mL/min for 12 h. Then the temperature was lowered to the reaction temperature, and syngas including 30%CO, $60\%H_2$, and $10\%N_2$ was introduced into the reactor. The reactor effluent gas was cooled to 273 K and separated into gas and liquid phases at reaction pressure. The gaseous products were directly analyzed on the on-line chromatograph through a sampling valve, and the liquid products were collected for a proper period with their weight measured, and subsequently analyzed on the chromatograph by injection. CO, CO_2, CH_4, and N_2 were directly analyzed using an on-line gas chromatograph (JIEDAO, GC-1690, thermal conductivity detector) equipped with a 3 m TDX-01 packed column through a sampling valve using H_2 as the carrier gas. Gaseous hydrocarbons were analyzed by an on-line gas chromatograph (JIEDAO, GC-1690, flame ionization detector (FID)) equipped with a 3 m Porapak Q packed column through a sampling valve with N_2 as the carrier gas. Liquid products were analyzed on the same FID chromatograph by injection. The concentration of hydrocarbons was calculated using pure CH_4 as standard gas, while that of the mixed alcohol was directly calculated from the peak area by using a standard liquid of higher alcohol. H_2O content in liquid product was analyzed using a moisture meter (ANTING, ZSD-2). Because the synthesis of higher alcohols requires an induction period to reach a steady-state condition, all activity data shown in this study were measured after the reaction was performed for more than 24 h.

DOI:10.1063/1674-0068/28/cjcp1504075

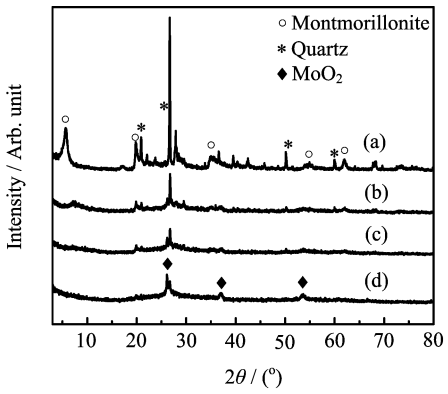

FIG. 1 XRD patterns of (a) clay and fresh K-Co-Mo/clay catalysts at different Mo/clay weight ratios of (b) 30%, (c) 50%, and (d) 70%.

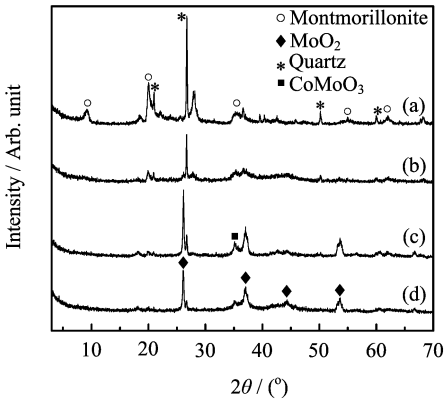

FIG. 2 XRD patterns of (a) reduced clay and reduced K-Co-Mo/clay catalysts at different Mo/clay weight ratios of (b) 30%, (c) 50%, and (d) 70%.

III. RESULTS AND DISCUSSION

A. XRD results

XRD patterns of fresh K-Co-Mo/clay catalysts at different weight ratios of Mo/clay are shown in Fig.1. For comparison, the diffraction patterns of the clay support was also listed. For the pristine clay, two main mineral phases: montmorillonite and quartz were identified. After the incorporation of active species, several new peaks assigned to MoO_2 species (2θ=26.1°, 37.0°, and 53.5°) were observed and no K-Mo or Co species were detected. The formation MoO_2 was attributed to the fact that in nitrogen, the decomposition of citric acid in the precursor gel partly reduced the Mo^{6+} to Mo^{4+} species [28]. Furthermore, the intensities of the diffraction peaks of MoO_2 species in the clay-supported catalysts were very weak, indicating that the active components had a high dispersion on the clay support surface. With an increase in the Mo loading, the intensity of clay peaks decreased while that of the MoO_2 peaks increased gradually. Furthermore, it is noted that the diffraction peak of clay at 2θ=5.6°, corresponding to the interlamellar spacing [29], shifted to higher 2θ values after impregnation with active components. These results indicated that incorporation of catalytic components decreased the interlamellar distance of clay. After reduction at 773 K, the diffraction peaks of MoO_2 became stronger and a new peak around 2θ=35.4° was observed (Fig.2), which may be assigned to $CoMoO_3$ species [28]. The results indicated that the reduction enhance the interaction between Co and Mo species.

B. N_2 adsorption-desorption results

Figure 3 shows the nitrogen adsorption-desorption isotherms and pore size distributions of the clay-supported K-Co-Mo catalysts with different Mo loading. For comparison purpose, the pristine clay support was also tested. The clay support exhibited a type IV isotherms with a hysteresis loop of type H3 according to the IUPAC classification [30]. This H3 type of a hysteresis loop was usually observed for solids consisting of agglomerates of particles forming conical-shaped pores. The pore size distribution curve indicated that the clay support possessed a mesoporous feature with a narrow size distribution. The clay-supported catalysts exhibited similar isotherms to that of the clay, suggesting that metal impregnation did not alter the pore structure of the parent support. At a high Mo loading of 70%, the condensation of adsorbates in the pores occurred at a relative pressure higher than that of other samples, indicating the presence of larger pores.

C. H_2-TPR results

The H_2-TPR profiles of the supported K-Co-Mo catalysts with the different weight ratios of Mo/clay and sole clay were presented in Fig.4. No obvious hydrogen consumption peak was observed for the sole clay support. After the incorporation of the catalytic components, two broad peaks at about 823 and 1033 K were assigned to the reduction of Mo^{6+} to Mo^{4+} and Mo^{4+} to $Mo^{\delta+}$, respectively [31]. The peak at 993 K corresponded to the reduction of Co^{2+} to Co^{+} species. With an increase in the Mo loading, the reduction peaks area became larger, indicating a higher H_2-consumption amount. Meanwhile, the reduction peak of Mo^{6+} to Mo^{4+} shifted to lower temperature, while that of Mo^{4+} to $Mo^{\delta+}$ and Co^{2+} to Co^{+} did not show significant change. The results indicated that increasing the Mo loading promoted the reduction of Mo^{6+} but had no significant influence on the reduction of Mo^{4+} and Co^{2+} species.

D. XPS results

The XPS spectra of Mo 3d for the fresh K-Co-Mo/clay catalysts with different Mo loading weight are

DOI:10.1063/1674-0068/28/cjcp1504075

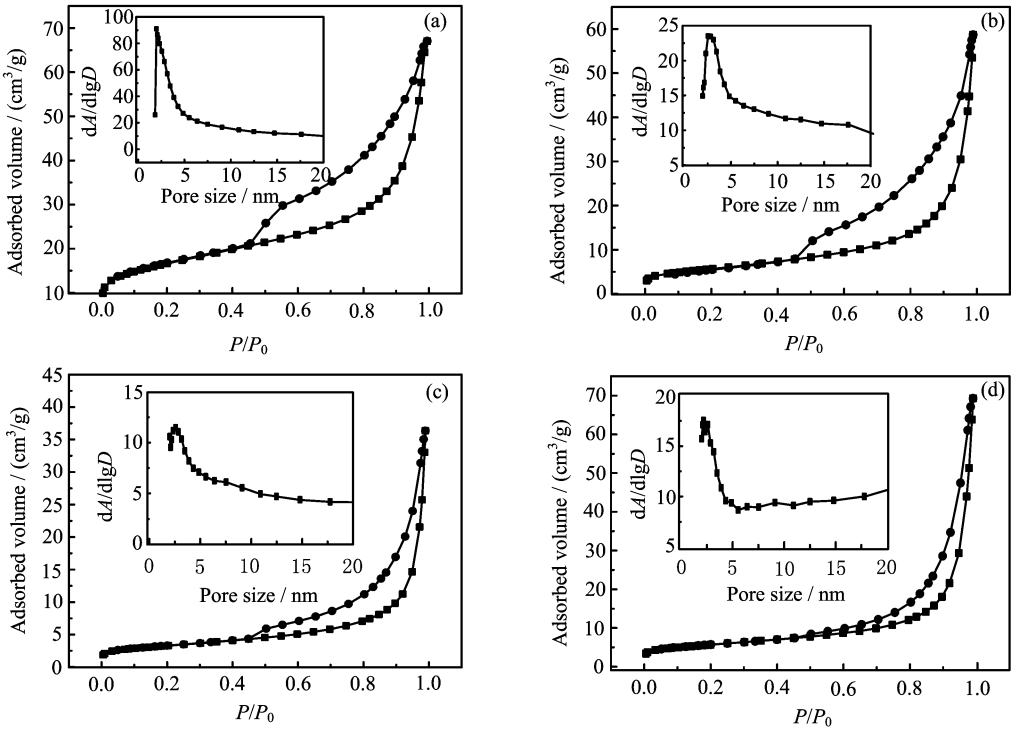

FIG. 3 Nitrogen adsorption-desorption isotherms of (a) clay, K-Co-Mo/clay catalysts at different Mo/clay weight ratios of (b) 30%, (c) 50%, and (d) 70%. Insert: pore size distribution curves.

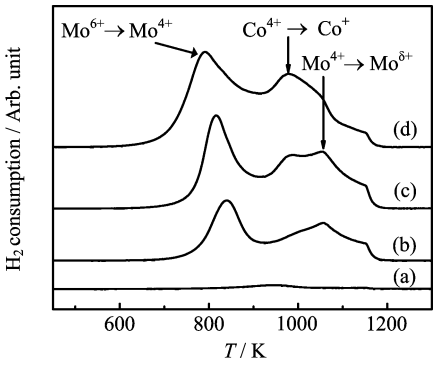

FIG. 4 H_2-TPR profiles of (a) clay and fresh K-Co-Mo/clay catalysts at different Mo/clay weight ratios of (b) 30%, (c) 50%, and (d) 70%.

shown in Fig.5. The Mo 3d spectra consisted of two peaks, a consequence of spin-orbit (j-j) coupling. The Mo $3d_{5/2}$ to $3d_{3/2}$ doublet were fitted so that each peak had the same Gaussian line shape and width. The relative area ratios of spinCorbit doublet peaks are 3/2, given by the ratio of their respective degeneracies ($2j$+1) [32]. A splitting energy of 3.15 eV was used for the Mo $3d_{5/2}$ to $3d_{3/2}$ doublet. The distribution of Mo species with different oxidation states and surface atomic ratio were calculated on the basis of the peak area.

From Fig.5, the characteristic binding energies E_b of Mo^{6+} $3d_{5/2}$ (232.5 eV), Mo^{6+} $3d_{3/2}$ (235.6 eV), Mo^{4+} $3d_{5/2}$ (230.8 eV), and Mo^{4+} $3d_{3/2}$ (234.0 eV) were observed. The distribution of Mo species with different oxidation states is presented in Table I. For the clay-supported catalysts, the percentage of surface Mo^{4+} species increased, while that of the Mo^{6+} decreased with an increase in the Mo loading. The result further provided evidence that an increase in the Mo loading can promote the reduction of Mo^{6+} species, as revealed by H_2-TPR result.

After reduction at 773 K, as shown in Fig.6, two new peaks at 229.3 and 232.4 eV were observed, which can be assigned to the characteristic binding energies of $Mo^{\delta+}$ ($1<\delta<4$) $3d_{5/2}$ and $3d_{3/2}$, respectively [32]. The distribution of Mo species with different oxidation state did not show significant change with an increase in the Mo loading. Figure 7 showed the surface atomic ratios of K/Mo and Co/Mo for the fresh and reduced clay-supported K-Co-Mo catalysts. With increasing the Mo loading, the surface K/Mo atomic ratios of the fresh and reduced K-Co-Mo/clay catalysts exhibited the same change trend. The reduction process promoted the enrichment of K on the catalyst surface. However, the Co/Mo atomic ratio had an opposite change trend for the fresh and reduced samples with an increase in the Mo loading. When the Mo loading exceeded 50%, the reduction treatment resulted in a decrease of surface Co species. The effects of reduction temperature on the Mo oxidation state are listed in Table II. For the cata-

DOI:10.1063/1674-0068/28/cjcp1504075

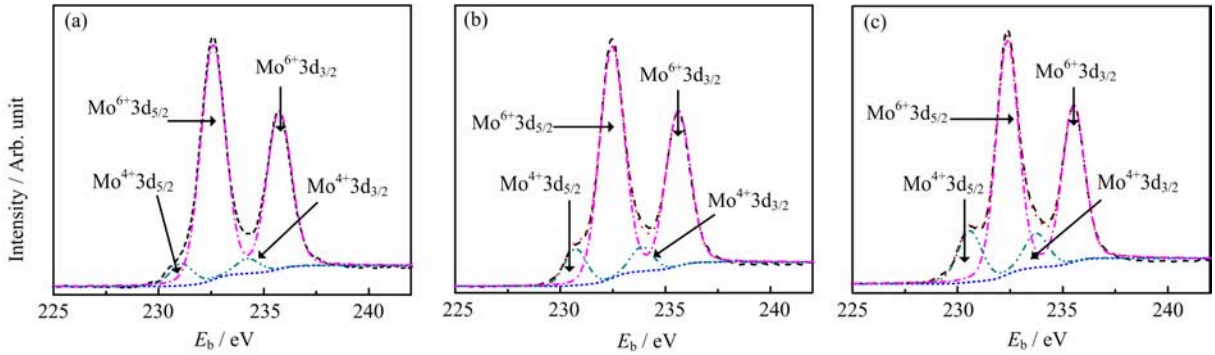

FIG. 5 XPS spectra of Mo 3d for fresh K-Co-Mo/clay catalysts at different Mo/clay weight ratios of (a) 30%, (b) 50%, and (c) 70%.

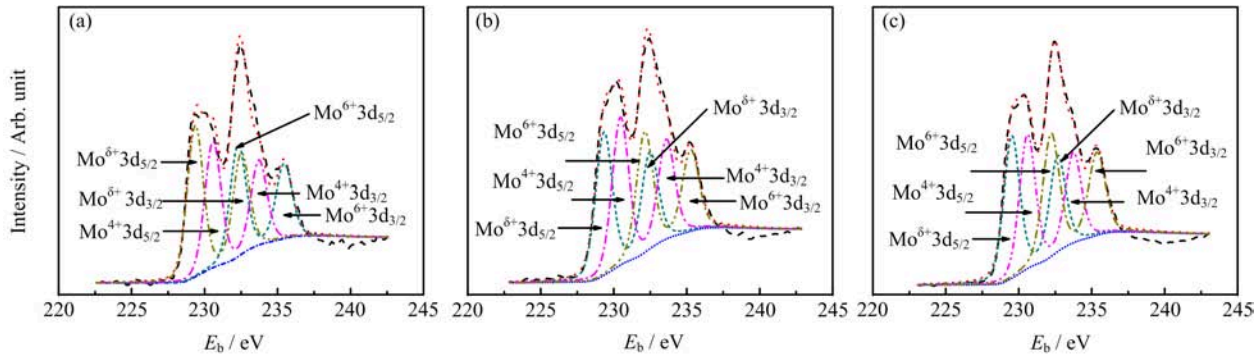

FIG. 6 XPS spectra of Mo 3d for reduced K-Co-Mo/clay catalysts at different Mo/clay weight ratio of (a) 30%, (b) 50%, (c) 70%.

TABLE I Distribution of surface Mo species for the fresh K-Co-Mo/clay catalysts with different Mo/clay weight ratios of 30%, 50%, and 70%.

Mo/clay	Mo^{4+}			Mo^{6+}		
	$E_b(3d_{5/2})$/eV	$E_b(3d_{3/2})$/eV	Percentage/%	$E_b(3d_{5/2})$/eV	$E_b(3d_{3/2})$/eV	Percentage/%
30%	230.8	234.0	8.5	232.5	235.6	91.5
50%	230.7	233.8	12.2	232.4	235.5	87.8
70%	230.6	233.7	19.2	232.3	235.4	80.8

lyst with Mo loading of 50%, the surface percentage of $Mo^{\delta+}$ increased with increasing the reduction temperature and reached a maximum value at 773 K. When further increasing the temperature, the content of $Mo^{\delta+}$ decreased, which may be attributed that the high temperature resulted in the sintering of particles and thus inhibited the reduction of Mo^{4+} species, as suggested by XRD results.

TABLE II Distribution of Mo species for K-Co-Mo/clay catalysts with Mo/clay weight ratio of 50% at different reduction temperatures (T).

T/K	Mo^{4+}/%	Mo^{6+}/%	$Mo^{\delta+}$/%
723	32.6	45.2	22.2
748	37.9	29.7	32.4
773	35.8	29.2	35.0
798	33.8	34.7	31.5

E. Catalytic performance

The catalytic performance of the clay-supported K-Co-Mo catalysts for higher alcohol synthesis from syngas are tested under the conditions of 553 K, 5.0 MPa, 4800 h^{-1}, and H_2 to CO molar ratio of 2. The activity data after an induction period of 24 h are listed in Table III. For comparison purposes, the unsupported K-Co-Mo catalyst with the same ratios of K/Mo and Co/Mo was tested under the same condition. It can be seen that the unsupported catalyst had a relatively low activity especially $C_{2+}OH$ selectivity for alcohol synthesis. The clay-supported K-Co-Mo catalysts showed a much higher catalytic performance than that of the

DOI:10.1063/1674-0068/28/cjcp1504075

TABLE III Effect of Mo loading and reduction temperature on the catalytic performance toward higher alcohol synthesis from syngas. Alc. STY: alcohol space-time-yield, Alc. sel.: alcohol selectivity.

	CO conv./C%	Alc. sel.[a]/C%	Alc. STY/(g/(kg·h))	C_nOH selectivity/C%				$C_1OH/C_{2+}OH$
				MeOH	EtOH	PrOH	BuOH	
(Mo/clay)/wt%								
30	13.0	44.7	40.8	22.9	12.8	6.9	2.1	1.05
50	22.5	48.0	98.6	15.9	12.4	14.6	5.0	0.50
70	27.7	48.3	105.8	19.2	15.7	8.4	4.9	0.66
Unsupported	28.5	40.3	64.2	18.9	11.8	7.5	1.9	0.88
T/K								
723	26.2	48.0	70.8	15.9	14.1	13.2	4.5	0.49
748	23.5	52.0	73.7	18.6	15.5	13.7	4.2	0.55
773	22.5	48.0	98.6	15.9	12.4	14.6	5.0	0.50
798	30.2	28.2	86.7	14.0	8.8	4.4	1.0	0.98

[a] Based on CO_2-free carbon atoms. Reaction conditions: T=553 K, P=5.0 MPa, GHSV=4800 h^{-1}, H_2/CO=2.

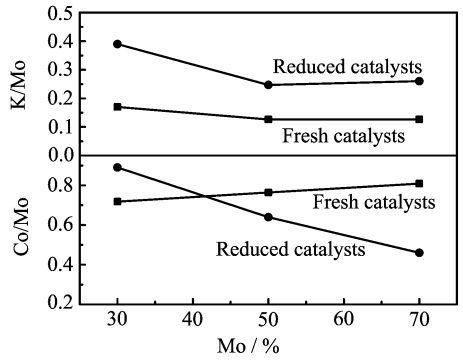

FIG. 7 Surface atomic ratios of K/Mo and Co/Mo of the fresh and reduced K-Co-Mo/clay catalysts at different Mo/clay weight ratios.

unsupported sample. On the catalyst with Mo loading of 50%, the STY of total alcohol reached 98.6 g/(kg·h), more than 50% higher than the unsupported sample. Especially the $C_1OH/C_{2+}OH$ ratio decreased significantly, from 0.88 to 0.50. Further increasing the Mo loading to 70%, the alcohol STY increased slightly, but the $C_{2+}OH$ content decreased significantly. The results indicated that the incorporation of clay as the support in the K-Co-Mo catalyst can enhance the activity for higher alcohol synthesis significantly. The effect of reduction temperature on the catalyst performance was also investigated. As shown in Table III, increasing the reduction temperature from 723 K to 773 K, the alcohol production, especially the $C_{2+}OH$ selectivity, increased significantly. Further increasing the reduction temperature, the catalyst performance decreased.

The properties of support has great influence on the alcohol synthesis from syngas [33]. Clays minerals, which are a class of two dimension layered structure and naturally-occurring minerals, were reported to be effective partial hydrogenation supports and have been extensively utilized in catalytic processes. The texture properties of the support such as pore size and mesoporosity has direct influence on the higher alcohol synthesis from syngas, which was associated with the reaction mechanism. The formation of higher alcohols on Mo-based catalyst consists of several steps: firstly the dissociation of adsorbed CO to form CH_2, followed by growth of alkyl chain via CH_2 insertion. Then the alkyl group reacted with nondissociatively adsorbed CO to form acyl species, which underwent further hydrogenation to form the higher alcohols [34]. From this point of view, the higher alcohols were secondary products and the alkyl group acted as the reaction intermediate. From the nitrogen adsorption-desorption results, the clay support had a large amount of narrow mesoporous structure, and the mesoporous structural integrity of the support remained unchanged after the impregnation of active species. Compared with the unsupported catalyst with very large pore size, the mesoporous structure of the supported catalyst is suggested to inhibit the mass diffusion of molecules to some extent [35]. As a consequence, the residence time of intermediates in the pore can be prolonged, which promoted the formation of higher alcohols. Similar conclusion was reported by Li *et al* [35]. They found that increasing the space velocity can suppress the formation of higher alcohols on the Mo-based catalyst. The reason can be due to the fact that a higher space velocity is associated with a lower residence time, which resulted in a larger fraction of the primary product and smaller fractions of secondary products. Besides, from the XRD results, the active components had a high dispersion on the clay support surface, which suggested that the supported catalyst had a high active surface area and also conductive to the alcohol synthesis. The XPS results indicated that after reduction, beside Mo^{6+} and Mo^{4+} species, a lower valence state $Mo^{\delta+}$ ($1<\delta<4$) species was observed. Muramatsu and Li *et al*. suggested that

DOI:10.1063/1674-0068/28/cjcp1504075

the $Mo^{\delta+}$ ($1<\delta<4$) species was the active site for the adsorption of nondissociative CO and responsible for the alcohol formation [34]. The *in situ* DRIFTS study in our previous work also confirmed the conclusion [28]. The formation of $Mo^{\delta+}$ ($1<\delta<4$) species can promote the adsorption of CO on the surface and favor the alcohol formation. The clay-supported catalysts performed the best activity at reduction temperature of 773 K, which may be attributed to the high content of $Mo^{\delta+}$ species on the surface.

IV. CONCLUSION

A kind of layered structure clay was incorporated as the support to prepare the K-Co-Mo catalyst by a sol-gel method. The active components had a high dispersion on the surface of clay support. The increase of the Mo loading can promote the reduction of Mo^{6+} but had no significant influence on the reduction of Mo^{4+} and Co^{2+} species. For the reduced samples, besides Mo^{6+} and Mo^{4+}, a kind of lower state $Mo^{\delta+}$ ($1<\delta<4$) species was observed on the surface, which was suggested to be responsible for the alcohol synthesis. Compared with the unsupported catalyst, the K-Co-Mo/clay showed much higher activity for alcohol formation. The reason was due to the fact that the supported catalyst have a high active surface area and the mesoporous structure is suggested to prolong the residence time of intermediates for alcohol formation in some extent, thus favoring the formation of higher alcohols. The catalyst reduced at 773 K showed the highest catalytic activity, which may be attributed to the high content of $Mo^{\delta+}$ species on the surface.

V. ACKNOWLEDGMENTS

This work was supported by the National Natural Science Foundation of China (No.11179034 and No.11205159) and the National Basic Research Program of China (No.2012CB922004).

[1] M. W. Barsoum, Prog. Solid State Chem. **28**, 201 (2000).
[2] K. G. Fang, D. B. Li, M. G. Lin, M. L. Xiang, W. Wei, and Y. H. Sun, Catal. Today **147**, 133 (2009).
[3] S. Zaman and K. J. Smith, Catal. Rev. **54**, 41 (2012).
[4] T. Toyoda, T. Minami, and E. W. Qian, Energy Fuels. **27**, 3769 (2013).
[5] D. Ferrari, G. Budroni, L. Bisson, N. J. Rane, B. D. Dickie, J. H. Kang, and S. J. Rozeveld, Appl. Catal. **462/463**, 302 (2013).
[6] V. P. Santos, B. van der Linden, A. Chojecki, G. Budroni, S. Corthals, H. Shibata, G. R. Meima, F. Kapteijn, M. Makkee, and J. Gascon, ACS Catal. **3**, 1634 (2013).
[7] K. Yin, H. Shou, D. Ferrari, C. W. Jones, and R. J. Davis, Top. Catal. **56**, 1740 (2013).
[8] D. A. Storm, Top. Catal. **2**, 91 (1995).
[9] M. Xiang, D. Li, W. Li, B. Zhong, and Y. Sun, Fuel **85**, 2662 (2006).
[10] V. R. Surisetty, A. K. Dalai, and J. Kozinski, Appl. Catal. **385**, 153 (2010).
[11] Z. Li, Y. Fu, J. Bao, M. Jiang, T. Hu, T. Liu, and Y. N. Xie, Appl. Catal. **220**, 21 (2001).
[12] J. Yu, D. Mao, G. Lu, Q. Guo, and L. Han, Catal. Comm. **24**, 25 (2012).
[13] V. R. Surisetty, J. Kozinski, and A. K. Dalai, J. Catal. **2013**, 1 (2013).
[14] Z. R. Li, Y. L. Fu, and M. Jiang, Appl. Catal. **187**, 187 (1999).
[15] B. M. Reddy, P. M. Sreekanth, Y. Yamada, and T. Kobayashi, J. Mol. Catal. **227**, 81 (2005).
[16] Y. A. Ryndin, R. F. Hicks, and A. T. Bell, J. Catal. **70**, 287 (1981).
[17] G. Z. Bian, L. Fan, Y. L. Fu, and K. Fujimoto, Ind. Eng. Chem. Res. **37**, 1736 (1998).
[18] H. Xiong, L. L. Jewell, and N. J. Coville, ACS Catal. **5**, 2640 (2015).
[19] V. R. Surisetty, A. Tavasoli, and A. K. Dalai, Appl. Catal. **365**, 243 (2009).
[20] M. T. Claure, S. H. Chai, S. Dai, K. A. Unocic, F. M. Alamgir, P. K. Agrawal, and C. W. Jones, J. Catal. **324**, 88 (2015).
[21] C. H. Zhou, Appl. Clay. Sci. **53**, 87 (2011).
[22] W. Wang, H. Liu, G. Ding, P. Zhang, T. Wu, T. Jiang, and B. Han, Chemcatchem **4**, 1836 (2012).
[23] A. Rinaldi, J. Zhang, J. Mizera, F. Girgsdies, N. Wang, S. B. Hamid, R. Schlogl, and D. S. Su, Chem. Comm. 6528, (2008).
[24] I. Jamshid, O. H. Donald, and T. Hossein, Appl. Catal. **231**, 99 (2002).
[25] I. Jamshid, T. Hossein, O. H. Donald, and N. Farhad, Fuel Process. Technol. **79**, 71 (2002).
[26] Y. Liu, K. Murata, M. Inaba, and R. Kinetics, Mech. Catal. **113**, 187 (2014).
[27] J. Bao, Y. L. Fu, and G. Z. Bian, Catal. Lett. **121**, 151 (2007).
[28] M. Zhang, W. Zhang, W. Xie, Z. Qi, G. Wu, M. Lv, S. Sun, and J. Bao, J. Mol. Catal. **395**, 269 (2014).
[29] N. Hamzah, N. M. Nordin, A. H. A. Nadzri, Y. A. Nik, M. B. Kassim, and M. A. Yarmo, Appl. Catal. **419/420**, 133 (2012).
[30] J. Rouquerol, D. Avniir, C. W. Fairbridge, D. H. Everett, J. H. Haynes, N. Pernicone, J. D. F. Ramsay, K. S. W. Sing, and K. K. Unger, Pure Appl. Chem. **66**, 1739 (1994).
[31] Y. Avila, C. Kappenstein, S. Pronier, and J. Barrault, Appl. Catal. **132**, 97 (1995).
[32] J. G. Choi and L. T. Thompson, Appl. Surf. Sci. **93**, 143 (1996).
[33] J. Wang, P. A. Chernavskii, Y. Wang, and A. Y. Khodakov, Fuel **103**, 1111 (2013).
[34] M. Atsushi, T. Takashi, and T. Hiro-o, J. Phys. Chem. **96**, 1334 (1992).
[35] L. Xianguo, F. Lijuan, and E. L. Kugler, Ind. Eng. Chem. Res. **37**, 3853 (1998).

DOI:10.1063/1674-0068/28/cjcp1504075